PERGAMON

Vision Research 38 (1998) 3735–3741

Vision Research

Elongated physiological summation pools in the human visual cortex[1]

Uri Polat [a,b], Anthony M. Norcia [a,*]

[a] *The Smith-Kettlewell Eye Research Institute, 2232 Webster Street, San Francisco, CA 94115, USA*
[b] *Institute for Vision Research, 14 Ehad Ha'am Street, Rehovot 76105, Israel*

Received 8 May 1997; received in revised form 25 November 1997

Abstract

The visibility of gratings improves with increasing stimulus area. This effect is usually interpreted as being due to probability summation between the outputs of linear, independent spatial filters, although non-linear spatial summation can have similar effects [1]. In order to distinguish between probabilistic and physiological summation models, we measured contrast thresholds using the Visual Evoked Potential (VEP). Our previous work [2] suggests that spatial summation in the VEP is nonlinear and that it occurs preferentially for collinear configurations. Traditional probability summation models predict that areal summation will improve threshold independent of stimulus configuration. Contrast thresholds were derived from VEP contrast response functions for either circular or elongated Gabor patches with aspect ratios up to 6:1. The carrier orientation was either the same as the patch envelope orientation (collinear) or orthogonal to it. Response amplitudes were larger and contrast sensitivity was higher for collinear configurations. The results are consistent with nonlinear, configuration dependent summation that is more extensive along the axis of orientation.

Keywords: Spatial summation; Long-range interactions; Evoked potential (EP); Facilitation; Inhibition; Contrast

1. Introduction

In the classical view of the organization of the visual cortex, afferent inputs are seen as flowing through hierarchically-organized stages, with each successive stage elaborating on the feature selectivity developed at earlier stages [3]. Classical receptive fields (CRF), tuned selectively for location, orientation and spatial frequency form the fundamental units of analysis in this view. During the time that the classical view of cortical physiology was developing, computational models of spatial vision were proposed that were based on linear spatial filters whose spatial weighting functions resembled those of cortical simple cells that possess 2–3 antagonistic spatial subunits [4–7]. In these models, the outputs of linear spatial filters produce a field of local signals that can be integrated at later stages of signal processing (e.g. [8–10]). It is common in filter-based models to include independent noise sources in the filters, and thus the sensitivity to extended stimuli increases as a probabilistic function of stimulus area. So-called probability summation models [11–13] can quite accurately predict the increase in sensitivity that occurs as the area of a grating patch is increased. These models, with their roots in linear systems theory, preserved two properties that are at the heart of the classical view of simple cells: linearity of spatial summation and a high degree of locality in the spatial domain.

However, the growth in visibility with increasing area can also be due to non-linear physiological summation [1]. Evidence is accumulating that spatial summation is non-linear, even in simple cells. Many laboratories ([14–17]; see also Ref. [18]) have found that the response to stimuli placed within the CRF of simple cells can be modified by stimuli placed outside of this region. Such effects can be either suppressive or facilitative [18]. Non-classical surround effects are, by definition, indicative of non-linear spatial summation. That is, the response of the cell to a combination of stimuli presented

* Correponding author. Fax: +1 415 5611610; e-mail: amn@skivs.ski.org.

[1] Preliminary results were reported at the 1996 Annual Meeting of the Society for Neuroscience: [50].

0042-6989/98/$19.00
PII: S0042-6989(97)00426-4

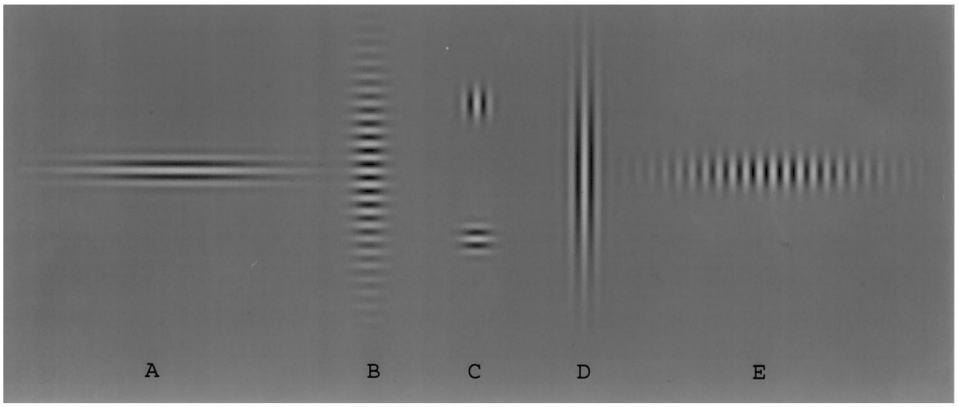

Fig. 1. Experimental stimuli. Gabor patches with 3 cd carriers were temporally modulated at 2.8 Hz in Onset/Offset mode. (A): Elongated Gabor patch ($0.3 \times 1.8°$ S.D.), aspect ratio = 6:1: collinear configuration. (B): Elongated Gabor patch, aspect ratio 6:1: orthogonal configuration. (C): Circular Gabor patches, aspect ratio = 1:1. (D): collinear configuration with carrier and envelope vertical. (E): Orthogonal configuration: carrier vertical, envelope horizontal.

inside and outside of its CRF cannot be predicted from the responses generated by the individual stimulus components.

Psychophysically, [19–21] have shown that spatial summation between multiple stimuli can be either facilitatory or inhibitory, depending on stimulus contrast and configuration. The visibility of a foveally viewed Gabor patch can be enhanced by the presence of similar patches presented at distances equivalent to several wavelengths of the Gabor carrier [19,20]. The enhancement of visibility is most prominent when the global orientation of the flanking patches matches that of the carrier. Similar effects have been seen in cat single-unit recordings where it was found that collinearly arranged targets placed in the non-classical surround of isolated single-units increased the cell's firing rate in the near threshold region [17,22]. Non-linear spatial interactions are also apparent in the human VEP. Polat and Norcia [2] have found that the amplitude of near threshold Gabor patches was enhanced by collinearly arranged Gabor patches placed up to 3° away. Orthogonally arranged flanks exerted a suppressive effect.

One implication of configuration specific, non-classical surround mechanisms is that spatial summation at contrast threshold may also be non-linear and configuration dependent. In the present experiments, we have used a VEP paradigm that is similar to previous psychophysical spatial summation paradigms and to the spatial interaction paradigm used in cat single-unit recordings [17,22] and in human VEP experiments [2]. The experiments involve deriving contrast thresholds from the VEP contrast response function as a function of stimulus area and configuration. We compared sensitivity for equal area targets expanded separately along the length and width axes. We chose to measure thresholds in order to relate the results to previous psychophysical studies of contrast threshold measured as a function of grating area [11–13,23,24]. The experiments differ from those of Polat and Sagi [19–21] in that the entire stimulus is presented at the same contrast: Polat and Sagi modified target threshold with suprathreshold lateral masks. The spatial interactions between the CRF and its surround [17,22] also involved suprathreshold stimulus elements, as did the VEP experiments of Polat and Norica [2]. In the present study, we find that response amplitudes are larger and contrast sensitivity is higher for Gabor patches that are elongated along the axis defined by the orientation of the carrier.

2. Methods

2.1. Observers

Nine observers with normal or corrected to normal vision in both eyes participated in these experiments. The experimental procedures were explained to the observers prior to participation in the experiment and each observer provided written informed consent.

2.2. Stimuli and experimental procedures

Foveally viewed circular and elongated Gabor patches were temporally modulated at 2.8 Hz in Onset/Offset mode with no change in space average luminance (100 cd/m^2). The Gabor patches consisted of a 3 c/deg cosine-phase grating, referred to as the carrier; see Fig. 1, multiplied by a two-dimensional Gaussian function envelope. Carrier contrast was incremented in ten equal logarithmic steps spanning the psychophysical threshold over the course of 10 s (contrast ranges spanned 3–4 octaves). An attenuation network [25] was used to combine three 8-bit video outputs to provide an effective 12 bits of contrast resolution after gamma correction. The aspect ratio of the Gabor patch was

controlled by varying the S.D. of the envelope along one axis, between 0.33 and 2.0°, while holding the standard deviation of the orthogonal axis constant at 0.33°. In this way we created patches with aspect ratios of 1:1, 2:1, 3:1, 4:1 and 6:1. The carrier orientation was either vertical or horizontal. In all experiments, the Gabor patches were presented in the center of a 13.8 × 10.4° field set to the mean luminance of the patches. Each condition consisted of 10–15 trials (10 s each), in which the spatial frequency of the carrier and orientation of both the carrier and the envelope were kept constant.

Trials were presented in blocks of 3–6 trials of the same condition, with the order of conditions being loosely randomized. A small, 2-arcmin fixation point was presented at the center of the screen, indicating the target location. When ready, the observers pushed a mouse key to start the trial. Observers were instructed to maintain fixation and to avoid eye movements.

2.3. VEP recording and signal processing

The electroencephalogram (EEG) was sampled at 397 Hz from a cruciform array of five electrodes centered at O_z and spaced by 3 cm. O_1, O_z and O_2 were used as were locations 3 cm up from O_z and 3 cm down from O_z, along the midline. All electrodes were referred to C_z. The amplitude and phase of the VEP at the first six harmonics of the stimulus frequency were extracted by a Recursive Least Squares adaptive filter [26]. The T^2_{Circ} statistic of Victor and Mast [27] was used to discriminate statistically significant driven activity from spontaneous EEG activity and for setting confidence limits on the response parameters. The VEP response to the small Gabor targets was dominated by the first harmonic, i.e. 2.8 Hz, in most observers. The second harmonic components were recordable in some observers, but the third and fourth harmonic components were only seen at high contrasts and only in some of the observers. The recording channel and response harmonic with the best threshold was selected for group data analyses. Contrast threshold was lowest at the first harmonic in approximately 80% of the records.

3. Results

Contrast response functions from observers UP and YP are presented in Fig. 2 for collinear (carrier and envelope, both vertical; circles) and orthogonal configurations (carrier horizontal, envelope vertical; squares). The aspect ratio was 6:1. VEP amplitude was a linear function of log stimulus contrast near threshold and extrapolation of the linear range to zero contrast yielded an estimated contrast threshold of 0.5%(UP) and 0.6%(YP) for the collinear and 0.8%(UP) and 1.4%(YP) for the orthogonal configuration (see arrows in Fig. 2). Statistically significant response amplitudes were recorded at lower contrasts in the collinear configuration and its contrast response function is shifted leftward over a range of contrasts above the estimated threshold (Error bars are ±1 S.E.M.)

Mean contrast sensitivity for seven observers as a function of aspect ratio is presented in Fig. 3 for collinear and orthogonal configurations. For the collinear configuration, sensitivity increased as a function of increasing area by more than 0.6 log units. For the orthogonal configuration, sensitivity improved by about 0.2 log units, saturating at an aspect ratio of 3:1. The results within the observer's ANOVA indicated significant main effects of carrier orientation or

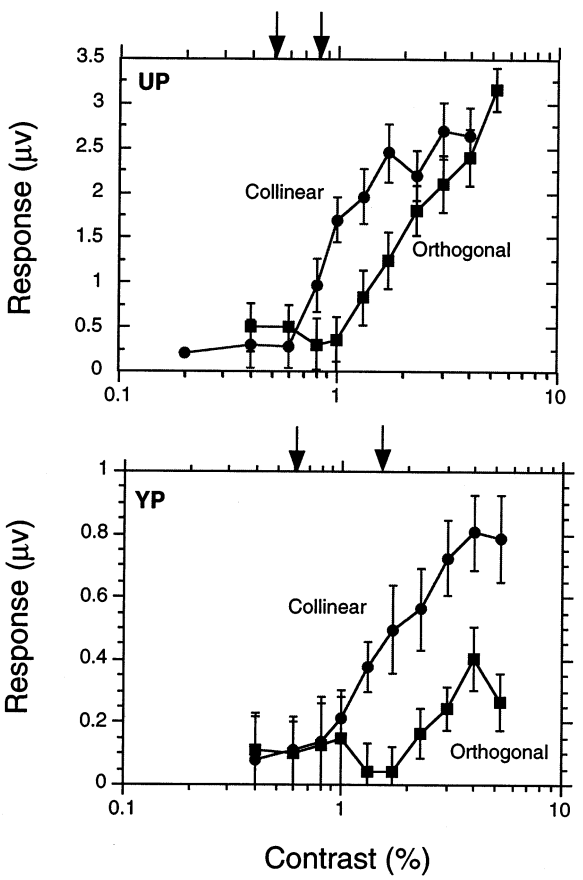

Fig. 2. Top panel. Contrast response functions for observer UP at an aspect ratio of 6:1. The Gabor envelope orientation was vertical and the carrier orientation was either vertical (collinear configuration; circles) or horizontal (orthogonal configuration; squares). Response amplitude is a linear function of log contrast at low contrasts. The contrast thresholds extrapolated from the linear range of the response function were 0.5% for the collinear versus 0.8% for the orthogonal configuration. The response amplitude is larger and the threshold is lower for the collinear configuration. Bottom panel. Contrast response functions for observer YP at an aspect ratio of 6:1 as in top panel. The contrast thresholds extrapolated from the linear range of the response function were 0.6% for the collinear versus 1.4% for the orthogonal configuration. The response amplitude is larger and the threshold is lower for the collinear configuration.

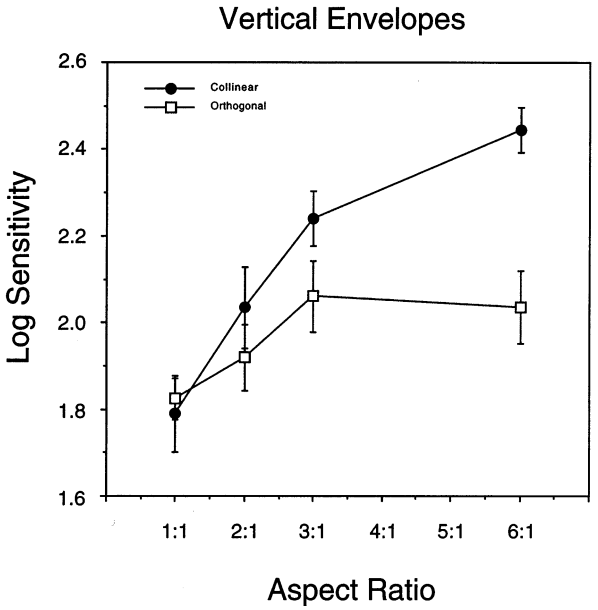

Fig. 3. Sensitivity versus aspect ratio: Constant envelope orientation (Vertical). Average data of seven observers. The sensitivity for the collinear configuration (circles) increased with increasing aspect ratio more than the orthogonal configuration (squares). Summation occurs up to an aspect ratio of at least 6:1. The 6:1 aspect ratio stimuli are represented in Fig. 1(B and D) for the orthogonal and collinear conditions, respectively.

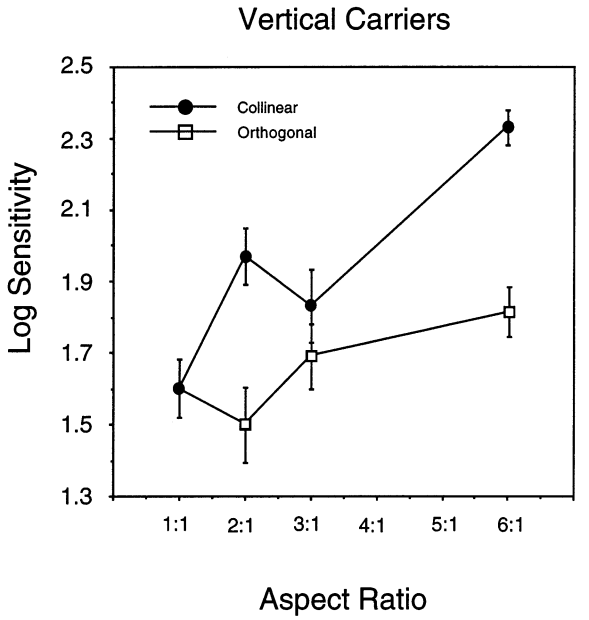

Fig. 4. Sensitivity versus aspect ratio: Constant carrier Orientation (Vertical). Average data of seven observers. Here the global orientation was either vertical or horizontal while the carrier orientation was kept constant (vertical). As in Fig. 3, sensitivity for the collinear configuration (circles) improved with increasing aspect ratio more than it did for the orthogonal configuration (squares). The 6:1 aspect ratio stimuli for this experiment are represented in Fig. 1(D and E) for the collinear and orthogonal conditions, respectively

configuration ($F = 18.07$; $P = 0.005$) and aspect ratio ($F = 13.7$; $P = 0.0001$) and a significant interaction between carrier orientation and aspect ratio ($F = 3.155$; $P = 0.05$).

To control for the effects of sensitivity differences that might exist between the vertical or horizontal carrier orientations, the next experiment kept the carrier orientation constant (vertical) and varied the envelope orientation (vertical and horizontal envelopes). Mean contrast sensitivities as a function of aspect ratio for seven observers are presented in Fig. 4. Similar to what was seen in Fig. 3, contrast sensitivity improved with increasing aspect ratio ($F = 7.9$; $P = 0.0065$). There was a main effect of envelope orientation ($F = 16.39$; $P = 0.0004$). There was also a significant interaction between aspect ratio and envelope orientation ($F = 2.9$; $P = 0.04$), with the vertical envelope (collinear) configuration leading to a steeper increase in sensitivity with increasing aspect ratio.

In the final experiment we measured contrast sensitivity for four collinear configurations (envelopes and carriers of the same orientation: vertical, horizontal and two diagonals) and for four orthogonal configurations (envelopes vertical, horizontal or oblique, with carriers of the orthogonal orientation). The aspect ratios were 1:1 and 4:1. Mean contrast sensitivity for six observers is shown as a function of configuration in Fig. 5. Contrast sensitivity was significantly higher for the collinear configurations ($F = 5.147$; $P = 0.04$), while no significant improvement was found for the orthogonal ones ($F = 2.24$; $P = 0.17$).

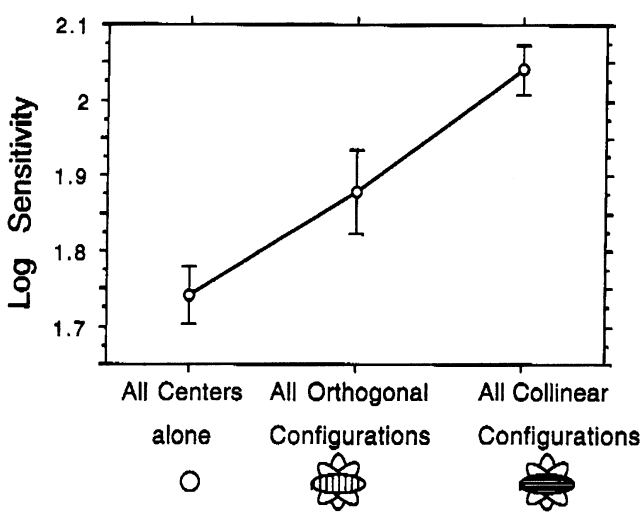

Fig. 5. Contrast sensitivity for four collinear configurations (envelopes and carriers of the same orientation: vertical, horizontal and two diagonals) and for four orthogonal configurations (envelopes vertical, horizontal or oblique, with carriers of the orthogonal orientation). The aspect ratios were 1:1 and 4:1. Mean contrast sensitivity for six observers is shown as as a function of configuration Contrast sensitivity was significantly higher for the collinear configurations, while non-significant improvement was found for the orthogonal ones.

4. Discussion

Increasing stimulus area produces configuration-specific improvements in contrast threshold—elongation of a grating along the orientation axis produced more physiological threshold summation than elongation along an orthogonal axis. Summation for the 3 c/deg carrier was observed up to a minimum aspect ratio of 6:1—or a distance equivalent to 12 grating cycles in the length direction at ± 1 S.D. The full extent of the VEP summation area is undoubtedly larger, since a clear saturation point was not reached in our experiments. Wright and Johnston [28] have found that VEP amplitude increases up to lengths that are equivalent to 9–16 grating cycles. Victor and Conte [29], using responses to iso-dipole textures have also identified a non-linear spatial pooling mechanism that also appears to be quite elongated.

Our summation experiments were designed to determine whether threshold summation occurs equally along the length and width dimensions of local oriented targets, as predicted by probability summation. Howell and Hess [11] measured length and width (cycle) summation psychophysically in separate experiments in two observers. The length summation experiment was done with patterns containing five grating cycles and the cycle summation experiment was done with an 'optimal length' grating determined from five cycle wide patterns. Apparently equivalent summation was observed for both dimensions and they concluded that the underlying detector was circularly organized and that probability summation across independent detectors was responsible for the improved visibility of extended targets. In our experiments, the basic summation mechanism underlying grating threshold is highly elongated. The Howell and Hess experiment did not specifically compare length and cycle summation at equivalent areas. Such a comparison is in principle possible retrospectively, but the available thresholds are substantially different for identical stimuli across their two experiments, making a more detailed comparison problematic. Our experiment has also emphasized the small-number-of-cycles regime which was not systematically explored in Howell and Hess who were interested in determining the number of cycles needed for complete summation in two dimensions. While probability summation cannot explain our configuration effect, it is possible that detection threshold for larger area gratings that are extended in both length and width is enhanced by probability summation among elongated filters. Watson et al. [23] found optimal contrast energy thresholds for a pattern that had the same extent (three cycles) in both length and width dimensions. They also manipulated the aspect ratio of their stimuli and compared patches elongated in both length and width dimensions. In their experiments, targets of comparable area that were elongated along the width or length axes produced comparable thresholds. Watson et al. [23] sampled only a few points in the two dimensional Fourier plane, whereas we have scanned both length and width dimensions in more detail. Polat and Tyler [24], using stimuli similar to those of the present study, have found that psychophysical detection threshold also improves more for Gabor patches elongated along the orientation axis than along the width axis.

The threshold summation areas seen in the present study are also substantially more elongated than those estimated in psychophysical masking studies. Spatial frequency masking data from Wilson's laboratory [7,30] places the aspect ratio of their 3 c/deg channel at 1.4:1. Daugman [31] estimated the elongation ratio of psychophysically defined channels at about 2:1, again based on masking data.

Our data are consistent with preferential physiological summation along the collinear direction that is mediated either by elongated CRFs or by configuration-specific, non-linear interactions between CRF mechanisms and their non-classical surrounds. Highly elongated CRFs are relatively uncommon in recordings from mammalian visual cortex that have used stimuli that are well above cellular threshold. Jones and Palmer [32] measured simple cell receptive field profiles using reverse correlation methods. Their simple cells were comprised of 2–3 spatial subunits whose aspect ratios ranged from 1.7:1 to 12:1. The most elongated receptive fields in their sample thus had aspect ratios of about 4:1. Several authors [33–36] have reported elongated receptive fields in layer six of cat striate cortex that may be comprised of pooled responses from smaller receptive fields in layer five. There are also reports of so-called periodic receptive fields that have multiple subunits along the width dimension. De-Valois et al. [37] found a small number of receptive fields that showed width summation up to seven cycles. However, 39 of 47 cells showed summation up to four or fewer cycles. Combined across studies, the average values of simple cell receptive field length-to-width elongation are about 1.5:1 ([32]; see also the summary in Ref. [38]) and are thus substantially less elongated than the summation areas we have found.

An alternative mechanism for configuration specific summation at threshold is the non-classical surround. Kapadia et al. [16] have found that collinear lines placed outside of the CRF preferentially enhance the response to an optimally oriented bar placed within the CRF. Similar effects have been observed with Gabor patches presented inside and outside the CRF of cat striate cortical neurons [17,22]. Moreover, Jagadeesh and Ferster [39] have shown that receptive field length in the primary visual cortex of cat is strongly dependent on stimulus contrast. They found that receptive field lengths could be up to five times longer when measured

with low contrast stimuli than with high contrast stimuli. Bosking and Fitzpatrick [40] have found cells in ferret visual cortex that show length summation for bar targets that extends well beyond the CRF. These non-classical surround effects indicate that spatial filtering by receptive fields is both non-linear and configuration specific.

Analogous 'collector' or 'collator' mechanisms have been proposed on the basis of psychophysical experiments [41–44]. Most relevant to the present experiments is Moulden's finding that the detectability of short, oriented line segments embedded in random distractor elements improves linearly as collinear elements are added, up to about seven elements. Performance improves beyond seven elements, but at a slower rate. Moulden [42] interpreted the initial phase as being due to physiological summation and the second phase as being due to probability summation among elongated, second-order collators. Summation in the present experiments occurred up to at least six wavelengths, but at a less than linear rate, e.g. the threshold did not improve 6 fold over a 6 fold increase in area. The increases seen lie between that expected from linear summation and from summation proportional to the square root of increasing area. Less than linear summation in our experiments may be due to the use of large 'elements' that extend well out of the foveola. One would expect that in our experiments, contrast sensitivity would not be uniform for each of the smaller elements contributing to the second order pool because of the relatively large retinal eccentricities involved (see Ref. [12]). This may reduce strength of summation seen in our experiments.

Both elongated classical and configuration specific, non-classical receptive field mechanisms may rely on long-range intrinsic connections [33,34] that tend to interconnect like-orientation columns. Bosking et al. [45] have shown recently that intrinsic connections in tree-shrew primary visual cortex are made preferentially among orientation columns that correspond to collinear stimuli in visual space. Similar anisotropies of axonal distribution have also been reported in a squirrel monkey [46] and in a cat [47]. Specificity in the spatial arrangement of local circuit axon arbors thus appears to play an important role in shaping the response properties of neurons in visual cortex [47,48].

VEP experiments cannot distinguish between summation within large CRFs and the effects of non-classical surrounds. Phenomenologically, the effects observed in the present experiment are similar to those seen by Jagadeesh and Ferster [39] and Polat et al. [17] in cat primary visual cortex. In each case cellular response for low contrast stimuli inside the receptive field was improved by collinear flanks in the non-classical surround. Non-classical surround mechanisms are known to be both spatial frequency and orientation selective [14] and configuration dependent [15,16,49]. Regardless of the underlying mechanism, our results very clearly suggest that orientation information is pooled preferentially along the orientation axis and that the pooling occurs over considerable distances.

Acknowledgements

This research was supported by grant EY06579 from the National Institutes of Health (A.M.N) and by a Rachel C. Atkinson Fellowship (U.P.)

References

[1] Graham NVS. Visual Pattern Analyzers. New York: Oxford University Press, 1989.
[2] Polat U, Norcia AM. Neurophysiological evidence for contrast dependent long range facilitation and suppression in the human visual cortex. Vis Res 1996;36:2099–109.
[3] Hubel DH, Wiesel TN. Receptive fields and functional architecture of monkey striate cortex. J Physiol Lond 1968;222:345–56.
[4] Marr D. Vision. San Francisco: WH Freeman, 1982.
[5] Watson AB. Summation of grating patches indicates many types of detectors at one retinal location. Vis Res 1982;22:17–25.
[6] Klein SA, Levi DM. Hyperacuity thresholds of 1 sec: theoretical predictions and empirical validation. J Opt Soc Am 1985;A2:1170–90.
[7] Wilson HR. Responses of spatial mechanisms can explain hyperacuity. Vis Res 1986;26:453–69.
[8] Wilson HR. Psychophysical models of spatial vision and hyperacuity. In: Regan D, editor. Vision and Visual Dysfunction Volume (10)-Spatial Vision. Boca Raton,FL: CRC Press, 1991:64–86.
[9] Adelson EH, Bergen JR. Spatiotemporal energy models for the perception of motion. J Opt Soc Am 1985;A2:285–99.
[10] Watt RJ, Morgan MJ. A theory of the primitive spatial code in human vision. Vis Res 1985;25:1661–74.
[11] Howell ER, Hess RF. The functional area for summation to threshold for sinusoidal gratings. Vis Res 1978;18:369–74.
[12] Robson JG, Graham N. Probability summation and regional variation in contrast sensitivity across the visual field. Vis Res 1981;21:409–18.
[13] Mayer MJ, Tyler CWT. Invariance of the psychometric function with spatial summation. J Opt Soc Am 1986;A3:1166–72.
[14] Maffei L, Fiorentini A. The unresponsive regions of visual cortical receptive fields. Vis Res 1976;16:1131–9.
[15] Nelson JI, Fiost BJ. Intracortical facilitation among cooriented, co-axially aligned simple cells in cat striate cortex. Exp Brain Res 1985;61:54–61.
[16] Kapadia MK, Ito M, Gilbert CD, Westheimer G. Improvement in visual sensitivity by changes in local context: parallel studies in human observers and in V1 of alert monkeys. Neuron 1995;15:843–56.
[17] Polat U, Mizobe K, Pettet MW, Kasamatsu T and Norcia AM. Collinear stimuli regulate visual responses depending on cell's contrast threshold. Nature 1998;391:580–84.
[18] Allman JM, Meizin F, McGuiness E. Stimulus specific responses from beyond the classical receptive field: neurophysiological mechanisms for local-global comparisons in visual neurons. Annu Rev Neurosci 1985;8:407–30.

[19] Polat U, Sagi D. Lateral interactions between spatial channels: suppression and facilitation revealed by lateral masking experiments. Vis Res 1993;33:993–9.
[20] Polat U, Sagi D. The architecture of perceptual spatial interactions. Vis Res 1994;34:73–8.
[21] Polat U, Sagi D. Spatial interactions in human vision: from near to far via experience-dependent cascades of connections. Proc Natl Acad Sci USA 1994;91:1206–9.
[22] Mizobe K, Kasamatsu T, Polat U, Norcia AM. Contrast and context modulation of single-cell responses elicited in cat area 17. Soc Neurosci Abstr 1996;22:642.
[23] Watson AB, Barlow HB, Robson JG. What does the eye see best? Nature 1983;302:419–22.
[24] Polat U, Tyler CW. What pattern the eye sees best? Vis Res (in press).
[25] Pelli DG, Zhang L. Accurate control of contrast on microcomputer displays. Vis Res 1991;31:1337–50.
[26] Tang Y, Norcia AM. An adaptive filter for steady-state evoked responses. Electroencephalogr Clin Neurophysiol 1995;96:268–77.
[27] Victor JD, Mast J. A new statistic for steady-state evoked potentials. Electroencephalogr Clin Neurophysiol 1991;78:378–88.
[28] Wright MJ, Johnston A. The effects of contrast and length of gratings on the visual evoked potential. Vis Res 1982;22:1389–99.
[29] Victor JD, Conte MM. Spatial organization of nonlinear interactions in form perception. Vis Res 1991;31(9):1457–88.
[30] Wilson HR, Gelb DJ. Modified line-element theory for spatial frequency and width discrimination. J Opt Soc America A. Opt Image Sci 1984;1:124–31.
[31] Daugman JG. Spatial visual channels in the Fourier plane. Vis Res 1984;24:890–1.
[32] Jones JP, Palmer LA. An evaluation of the two-dimensional Gabor filter model of simple receptive fields in cat striate cortex. J Neurophysiol 1987;58:1233–58.
[33] Gilbert CD, Wiesel TN. Intrinsic connectivity and receptive field properties in visual cortex. Vis Res 1985;25:365–74.
[34] Bolz J, Gilbert CD. The role of horizontal connections in generating long receptive fields in the cat visual cortex. Eur J Neurosci 1989;1:263–8.
[35] Schwarz C, Bolz J. Functional specificity of long-range horizontal connection in cat visual cortex: a cross-correlation study. J Neurosci 1991;11:2995–3007.
[36] DeAngelis GC, Freeman RD, Ohzawa I. Length and width tuning of neurons in the cat's primary visual cortex. J Neurophysiol 1994;71:347–74.
[37] De Valois RL, Thorell LG, Albrecht DG. Periodicity of striate cortex-cell receptive fields. J Opt Soc Am 1985;A2:1115–23.
[38] Daugman JG. Uncertainty relation for resolution in space, spatial frequency, and orientation optimized by two-dimensional visual cortical filters. J Opt Soc Am A. Opt Image Sci 1985;2:1160–9.
[39] Jagadeesh B, Ferster D. Receptive field lengths in cat striate cortex can increase with decreasing stimulus contrast. Soc Neurosci Abstr 1990;16:293.
[40] Bosking WH, Fitzpatrick D. Physiological correlates of anisotropy in horizontal connections: length summation properties of neurons in layers 2 and 3 of tree shrew striate cortex. Soc Neurosci Abstr 1995;21:1751.
[41] Morgan MJ, Hotopf WHN. Perceived diagonals in grids and lattices. Vis Res 1989;29:1005–15.
[42] Moulden B. Collator units: second stage orientational filters. In: Ciba Foundation Symposium 184 (editor). Higher-order Processing in the Visual System. Chichester: Wiley, 1994.
[43] Levi DM, Waugh SJ. Position acuity with opposite-contrast polarity features: evidence for a nonlinear collector mechanism for position acuity? Vis Res 1996;36:573–88.
[44] Mussap AJ, Levi DM. Spatial properties of filters underlying vernier acuity revealed by masking: evidence for collator mechanisms. Vis Res 1996;36:2459–73.
[45] Bosking WH, Zhang Y, Schofield B, Fitzpatrick D. Orientation selectivity and the arrangement of horizontal connections in tree shrew striate cortex. J Neurosci 1997;15:2112–27.
[46] Sincich L, Blaisdel GG. Lateral connections and orientation preference in layers II/III of squirrel monkey striate cortex. Soc Neurosci Abstr 1995;21:393.
[47] Schmidt KE, Goebel R, Lowel S, Singer W. The perceptual grouping criterion of colinearity is reflected by anisotropies of connections in the primary visual cortex. Eur J Neurosci 1997;9:1083–9.
[48] Fitzpatrick D. The functional organization of local circuits in visual cortex: insights from the study of tree shrew striate cortex. Cereb Cortex 1996;6:329–41.
[49] Grinvald A, Lieke EE, Frostig RD, Hildesheim R. Cortical point-spread function and long range interactions revealed by real-time optical imaging of macaque monkey primary visual cortex. J Neurosci 1994;14:2545–68.
[50] Polat UP, Norcia AM. Configuration-dependent physiological summation in human foveal visual. Soc Neurosci Abstr 1996;22:887.